ALCHEMY Jurnal Penelitian Kimia

Official Website: https://jurnal.uns.ac.id/alchemy

ISSN 1412-4092
EISSN 2443-4183

Improvement of Selectivity and Antifouling Properties of Chitosan-modified Polyvinylidene Fluoride (PVDF) Membrane for Protein Filtration

Reza Zatadini[a], Aldita Fatchul Ni'mah[a], Yudi Setiawan[a], Agung Lucky Pradita[a], Desy Vita Pratiwi[a], Dina Syakirina[a], Mayzy Vanesia Insani[a], Widyan Muhammad Naufal[a], Wulida Rayhani[a], Ozi Adi Saputra[b,c], Edi Pramono[a*]

[a]*Department of Chemistry, Faculty of Mathematics and Natural Sciences, Universitas Sebelas Maret*
Jalan Ir. Sutami 36 A, Kentingan, Surakarta, 57126, Indonesia
[b]*Sustainable Chemical Science and Technology, Taiwan International Graduate Program, and Institute of Chemistry, Academia Sinica*
Taipei, 11529, Taiwan
[c]*Department of Chemical Engineering, Collage of Engineering National Taiwan University*
Taipei, 10617, Taiwan

[*]*Corresponding author: edi.pramono.uns@staff.uns.ac.id*

DOI: 10.20961/alchemy.19.2.72110.210-222

Received 8 March 2023, Revised 8 June 2023, Accepted 10 June 2023, Published 30 September 2023

Keywords:

albumin;
bovine serum;
chitosan;
membrane technology;
protein filtration;
PVDF.

ABSTRACT. Protein with high purity is currently a valuable commercial commodity, prized for its high value and application in specialized functions. PVDF-based membrane technology has found widespread use in protein purification processes. However, the issue of fouling on the membrane surface frequently hampers the performance of PVDF membranes. The present study aims to enhance PVDF membranes' selectivity and antifouling properties through chitosan modification, thereby optimizing protein filtration. PVDF and PVDF/Chitosan membranes were fabricated using the phase inversion technique, followed by a comprehensive characterization of their surface properties, thermal attributes, and performance in bovine serum albumin (BSA) protein filtration. The collected data revealed notable increases in membrane hydrophilicity, porosity, and pure water flux due to the incorporation of chitosan. The membrane protein rejection capabilities were significantly enhanced to levels exceeding 90% with the introduction of 0.5% chitosan. Moreover, as the chitosan concentration increased, the membrane exhibited superior antifouling characteristics, with the 0.5% chitosan concentration yielding the highest Flux Recovery Ratio (FRR) value of 85.35%. Considering the significant improvement selectivity and antifouling properties in the combined system, the chitosan-modified PVDF membrane holds substantial promise in protein purification applications.

INTRODUCTION

The demand for protein of impeccable purity and devoid of microorganisms has become imperative in medical applications (Japranata, 2016). The industrial technology, particularly protein separation, remains challenging yet ever-evolving. Membrane technology has emerged over the past few years as a noteworthy alternative within the spectrum of protein separation and purification (Nunes *et al.*, 2020). Membrane filtration stands out as a premier technique due to its ability to uphold proteins' functional and nutritional attributes. Membrane filtration has numerous advantages, encompassing high selectivity, rapidity, cost-effectiveness, facile fabrication, minimal energy consumption, heightened efficiency, and the generation of top-tier quality permeate (Ezugbe *and* Rathilal, 2020; Gifuni *et al.*, 2020).

Membranes can be fabricated from both inorganic and organic polymeric materials, including but not limited to polyvinyl pyrrolidone (PVP), polyaniline, polysulfone (PSF), polyethersulfone (PES), cellulose acetate, polyacrylonitrile (PAN), polyamide (PA), polyimide (PI), polytetrafluoroethylene (PTFE), and polyvinylidene fluoride (PVDF) (Khajouei *et al.*, 2018; Shahrabi *et al.*, 2018; Ashok *et al.*, 2019; Chong *and* Wang, 2019; Khumalo *et al.*, 2019; Abriyanto, 2021). Among these, PVDF stands out, being extensively employed as the primary membrane material due to its remarkable attributes of high mechanical strength, thermal stability, and

Cite this as: Zatadini, R., Ni'mah, A. F., Setiawan, Y., Pradita, A. L., Pratiwi, D. V., Syakirina, D., Insani, M. V., Naufal, W. M., Rayhani, W., Saputra, O. A., and Pramono, E., 2023. Improvement of Selectivity and Antifouling Properties of Polyvinylidene Fluoride (PVDF) Membrane with Chitosan Modification for Protein Filtration. *ALCHEMY Jurnal Penelitian Kimia*, 19(2), 210-222. https://dx.doi.org/10.20961/alchemy.19.2.72110.210-222.

chemical resistance (Silitonga *et al.*, 2018). In general, PVDF membranes are prevalent in various filtration processes, namely ultrafiltration (UF), microfiltration (MF), nanofiltration (NF), and reverse osmosis (RO) (Elizalde *et al.*, 2018). Their applications are extensive, ranging from wastewater treatment, dye filtration, and removal of pollutants from water (e.g., boron, volatile organic compounds, and ammonia) to protein filtration in hemodialysis (Kang *and* Cao, 2014; Ezugbe *and* Rathilal, 2020; Nunes *et al.*, 2020; Yusuf *et al.*, 2020). Nevertheless, PVDF exhibits inadequate membrane hemocompatibility and inherent hydrophobicity, which can lead to membrane fouling or clogging (Liu *et al.*, 2019). Thus, fouling mitigation on the membrane surface involves blending hydrophilic polymers with hydrophobic polymers during the membrane fabrication (Liu *et al.*, 2019; Lusiana *et al.*,2020).

Chitosan is a hydrophilic polymer derived from chitin through a deacetylation process, with attributes like hydrophilicity, biodegradability, non-toxicity, biocompatibility, antibacterial properties, and human body safety. The hydroxyl (−OH) and amine ($-NH_2$) groups within chitosan confer hydrophilic and facilitate convenient chemical modifications (Lusiana *et al.*, 2020). Chitosan has been widely used as a filler to improve the hydrophilicity of various membrane materials (Lusiana *et al.*, 2020; Khabibi *et al.*, 2021). In the context of PVDF, the introduction of modified chitosan has found utility in diverse arenas, for example, including removing direct blue 14 dye (Hassanzadeh *et al.*, 2021), separation of Cr(IV) ions (Pishnamazi *et al.*, 2020), and removing volatile harmful organic compounds from water (Al-Gharabli *et al.*, 2023). Despite these versatile uses, chitosan's potential as a PVDF membrane filler for protein filtration remains unexplored.

Hence, the present study delves into modifying the PVDF membrane with chitosan and evaluates its efficacy in protein filtration and antifouling performance. The fabrication of membranes followed the phase inversion method, and the PVDF/Chitosan modified membrane underwent a comprehensive assessment of its surface properties, thermal properties, and bovine serum albumin (BSA) separation ability.

RESEARCH METHODS

The tools used in this research include analytical balance (BOECO Germany Max 120 g), dead-end filtration device with stirring cell, thickness gauge, compressor (Lakoni Fresco- 260X), Fourier Transform Infrared (FTIR) Shimadzu IR Prestige-21, Attenuated Total Reflection-Fourier Transform Infrared (ATR-FTIR) Agilent cary60, Oven (Memmert Atmosafe UN30-1060 E7086), X-Ray Diffraction (XRD Bruker D8 Advance), UV-Vis spectrophotometer (Hitachi), and ImageJ for image processing. The materials used are chitin (Nitra Kimia), polyvinylidene fluoride (PVDFSolef1010; Mw 352,000 g/mol, Solvay®), polyethylene glycol 200 (PEG200, Merck), N, N-Dimethylacetamide for synthesis 127-19-5 (DMAc) (Merck), NaOH pellets for analysis 1310-73-2 (Merck), bovine serum albumin (BSA) (Nitra Kimia), and distilled water (Cipta Kimia).

Deacetylation of Chitosan

Deacetylation of chitosan was carried out based on previous research (Trung *et al.*, 2006). This process aims to change chitin into chitosan. Chitin powder was refluxed in NaOH 50% with a ratio of chitin and NaOH is 1:10 (%wt/v) for 20 hours at 65 °C and neutralized using distilled water. The solid was filtered and dried at room temperature.

Fabrication of PVDF/Chitosan Membrane

The membrane fabrication used the phase inversion method based on previous research (Pramono *et al.*, 2022). Chitosan with a certain weight was dispersed in DMAc for 10 minutes. After that, PEG200 and PVDF were added into the suspension and stirred for 24 hours at 60 °C. The composition of the casting solutions with total mass 12 grams is shown in Table 1. The casting solution was poured on a glass plate and immersed in a water coagulant bath. The resulting membrane was taken and stored in a glycerin solution for further analysis.

Table 1. Membrane matrix composition.

Membrane	PVDF (wt%)	Chitosan (wt%)	PEG200 (wt%)	DMAc (wt%)
PVDF	18	-	4	78.0
PCs 0.3%	18	0.3	4	77.7
PCs 0.5%	18	0.5	4	77.5
PCs 1%	18	1.0	4	77.0

Characterization

Degree of Deacetylation Analysis

The deacetylation degree (DD) and functional groups of chitosan were analyzed using a Fourier Transform Infrared Spectroscopy (FTIR) with potassium bromide (KBr) pellet and calculated in Equation (1) (Khan *et al.*, 2002).

$$DD = 100 - [(A_{1655} / A_{3450}) \times 115] \quad (1)$$

where A_{1655} and A_{3450} were the absorbances at 1655 cm^{-1} of the amide-I band as a measure of the N-acetyl group content and 3450 cm^{-1} of the hydroxyl band as an internal standard to correct for film thickness or differences in chitosan concentration powder form. The factor '115' denoted the value of the ratio of A_{1655}/A_{3450} for fully N-acetylated chitosan. It was assumed that the value of this ratio was zero for fully deacetylated chitosan, and there was a rectilinear relationship between the N-acetyl group content and the absorbance of the amide-I band.

ATR-FTIR Characterization

The α- and β-phase polymorphs in PVDF were identified using an Attenuated Total Reflection-Fourier Transform Infrared (ATR-FTIR) with an accumulation of 48 scans and a resolution of 4 cm^{-1}. The β phase fraction (F(β)) was calculated using Equation (2).

$$F(\beta) = \frac{A_\beta}{\left(\frac{K_\beta}{K_\alpha}\right)A_\alpha + A_\beta} \quad (2)$$

with A_α and A_β being the α- and β-phase absorption peaks at 763 cm^{-1} and 840 cm^{-1}, respectively. K_α and K_β are the absorbance coefficients, which are 6.1 x 10^4 cm^2/mol and 7.7 x 10^4 cm^2/mol, respectively (Pramono *et al.*, 2022).

Membrane Structure Analysis

The membrane structure was analyzed using an X-ray diffraction (XRD) instrument with a scanning speed of 0.02°/min and a specimen scanning range of 2θ = 10° – 90°. The analysis was carried out to identify the phases of PVDF and chitosan. The data obtained were evaluated with Bruker D8 Advance XRD software, and further analysis was performed with Origin 2018 software.

Thermal Properties Analysis of Membranes

The thermal properties of the membrane were analyzed using a Simultaneous Thermal Analysis (STA). Thermal measurements were performed with a TGA-DSC type S thermocouple with an alumina crucible and air atmosphere. Membrane samples were burned at a heating rate of 10°/minute in the temperature range of 25 – 900 °C. The obtained data were evaluated with STA Linseis PT1600 software, and further analysis was performed with Origin 2018 software.

Hydrophilicity Analysis of Membranes

Membrane hydrophilicity was determined using the water contact angle (Pramono *et al.*, 2022). Water drops on the membrane surface were made and recorded with a macro camera. The images were taken and analyzed with ImageJ software in contact angle plugin mode. Each sample was measured with five repetitions with different positions of water droplets on the membrane, and the final data is the average value.

Porosity Analysis of Membranes

The porosity of the membrane was measured by gravimetric following the previous report (Pramono *et al.*, 2022). Membranes with dimensions of 2 × 2 cm were soaked in distilled water, dried with tissue, and then weighed as the wet weight of the membrane. The membrane was dried in an oven at 60 °C for 24 hours. The dried membrane was weighed, and the thickness of the dried membrane was measured. Membrane porosity was calculated using Equation (3).

$$\varepsilon(\%) = \frac{W_b - W_k}{A \times l \times \rho} \quad (3)$$

where W_b is the wet weight of the membrane, W_k is the dried weight of the membrane, l is the membrane thickness, A (cm^2) is the surface area of the membrane, and ρ is the density of water (0.998 g/cm^3).

Analysis of Membrane Performance Toward Filtration of Bovine Serum Albumin (BSA)

Membrane performance toward bovine serum albumin (BSA) feed solution followed the previous report (An *et al.*, 2017), using a dead-end ultrafiltration system. The membrane performance was analyzed in three stages: determination of pure water flux, BSA rejection, and antifouling analysis. The experiment was conducted at a temperature of 25 °C and dead-end pressure of 2 bar. Determination of pure water flux was carried out by installing a 5 cm diameter membrane sample on the system. The system was filled with distilled water as feed, and permeate was collected after 15 min compaction. The permeate was collected, and the water flux was determined by Equation (4). Membrane rejection was carried out at a later stage by replacing the feed using 100 mg/L BSA solution and analyzed again for 15 minutes. The membrane rejection was determined by Equation (5).

$$J = \frac{V}{\Delta t \times A} \quad (4)$$

$$R(\%) = \left(1 - \frac{C_p}{C_r}\right) \times 100 \quad (5)$$

J represents the permeation flux (L/m^{2}h) for water; V is the volume of permeate solution (L); A is the membrane area (m^2); and t is the permeation time. Rejection (R%) was obtained using permeate solution concentration (C_p) and feed solution concentration (C_r) measured using a UV-Vis spectrophotometer with a wavelength of 280 nm (Boributh *et al.*, 2009).

Determination of the antifouling properties by measuring the flux recovery ratio (FRR) of the membrane was carried out at the last stage. After performing the flux determination of pure water and BSA, the membrane was washed with water. The membrane is installed on the system and filled with distilled water as feed, the permeate is collected, and the FRR of the membrane is determined by Equation (6).

$$FRR(\%) = \frac{J_n}{J_0} \times 100 \quad (6)$$

J_0 represents the permeation flux (L/m^{2}h) for water, and J_n represents the permeation flux (L/m^{2}h) after being passed by BSA filtration.

RESULTS AND DISCUSSION

Deacetylation of Chitosan

The augmentation of the chitosan deacetylation degree was executed through a reaction with NaOH solution, as shown in Figure 1a. This process employed NaOH to catalyze the hydrolysis of chitin, transforming it into chitosan. Within the deacetylation process, the linkage between carbon within acetyl groups and nitrogen is disrupted, resulting in the formation of amine groups (Azizati, 2019). The intricate mechanism of this reaction is illustrated in Figure 1b.

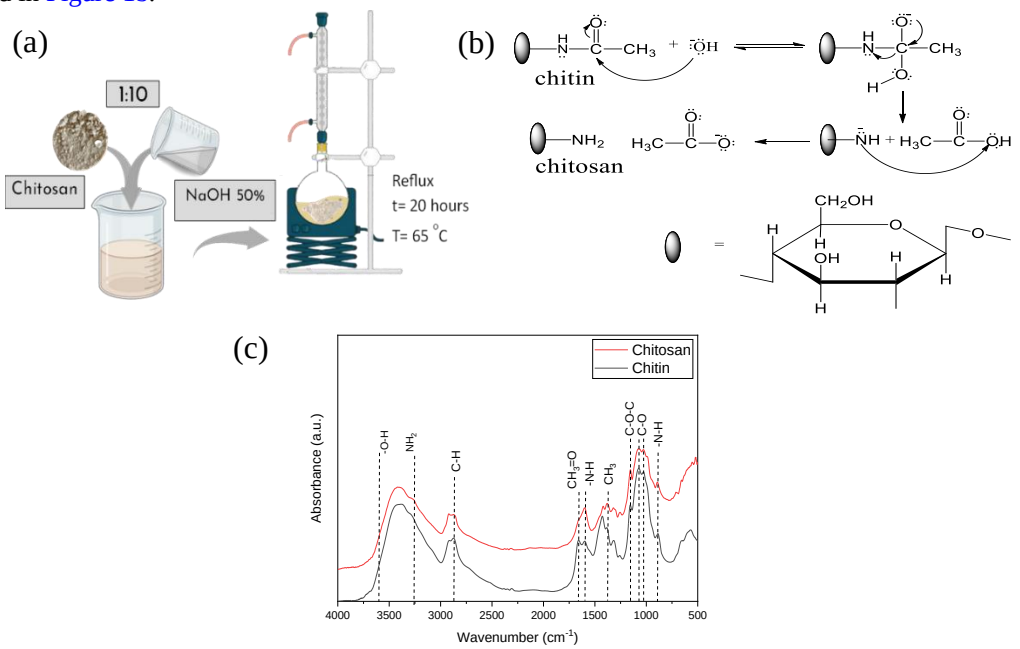

Figure 1. Illustration of (a) chitosan deacetylation process, (b) mechanism of chitosan deacetylation reaction (Azizati, 2019), and (c) FTIR spectra of chitin and chitosan.

The results of the FTIR functional group analysis on the deacetylation product are given in Figure 1c. The process led to the removal of acetyl groups from chitin, evident by the attenuation of the peak at 1659 cm^{-1}. The emergence of absorption at 1600 cm^{-1}, corresponding to the N-H bending vibration of $R–NH_2$, stands as evidence of the successful deacetylation process (Junaidi *and* Rahmadani, 2008).

FTIR spectrum of chitosan exhibits absorption at 894 cm^{-1} and 1157 cm^{-1}, corresponding to N–H wagging and =C–O–C stretch vibration, respectively. The peaks at 1031 cm^{-1} and 1073 cm^{-1} indicate the –C–O strain in cyclic alcohols, while 1379 cm^{-1} absorption is linked to the symmetric deformation of CH_3. A distinctive absorption at 1600 cm^{-1} signifies the characteristic absorption of –N–H deformation in amino groups. The absorption at 2871 cm^{-1} is likely an asymmetric C–H stretch, whereas the broad and strong absorption from 3260 cm^{-1} to 3600 cm^{-1} is an asymmetric stretch of –O–H and $–NH_2$ groups (intramolecular hydrogen bonds) in chitosan (Boributh *et al.*, 2009; Hassanzadeh *et al.*, 2021). The results of the FTIR analysis affirm the successful execution of the deacetylation process, as evident from the elevated DD value, ascending from 60.2% to 80.5%. Notably, the DD value usually ranges between 40% to 75% for chitin-chitosan conversion, while commercial chitosan commonly exhibits DD value between 70% – 90% (Kou *et al.*, 2021).

Membranes Characterization

Fabrication of PVDF/Chitosan membranes was carried out using the phase inversion method. The preliminary characterization of PVDF and PVDF/Chitosan membranes encompassed the use of ATR-FTIR, with the findings depicted in Figure 2a. The absorption at 761 cm^{-1} and 842 cm^{-1} indicates the α and β phases of the membranes, respectively (Dong *et al.*, 2014). The phase inversion method commonly instigates the formation of α and β phases in PVDF (Zheng *et al.*, 2018). The absorption of $–CF_2$ and C=C stretches of PVDF are shown at 1180 and 1405 cm^{-1}, respectively. The PVDF/Chitosan membrane has an absorption at 900 cm^{-1} and 1068 cm^{-1}, which is the –N–H wagging and –C–O stretching in cyclic alcohols (Boributh *et al.*, 2009). Subsequent to the incorporation of 0.5% chitosan, the absorbance peaks at 1111 cm^{-1} and 994 cm^{-1} emerged, signifying the presence of C–O–C bonds in cyclic alcohols (Fernandes *et al.*, 2015; Munim *et al.*, 2020). The β fraction value of PVDF after chitosan addition was calculated with Equation (3), as shown in Figure 2b. The introduction of hydrophilic polymers can enhance the beta fraction within PVDF membranes, as demonstrated by Pramono *et al*. (2022), where cellulose fillers elevated the β fraction to 58.8% in PVDF membranes. Consequently, chitosan emerges as a factor capable of orienting the PVDF polymer structure towards the more polar β phase.

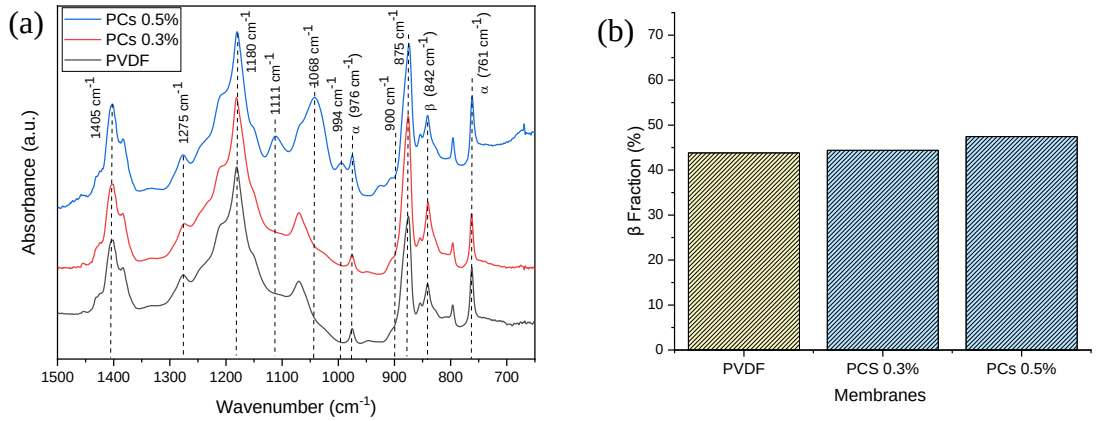

Figure 2. Spectra of (a) ATR-FTIR and graph of (b) β fraction of the membranes.

Figure 3 depicts the XRD diffractograms of both PVDF and PVDF/Chitosan membranes. The data showed distinctive 2θ peaks: 20° for the α phase, 18.3° and 19.9° for the α and γ phases, and 20.02° for the β phase (Thakur *et al.*, 2014; Zhao *et al.*, 2016). XRD of chitosan shows a 2θ peak at 20.19°, attributed to intermolecular and intramolecular hydrogen bonds between amino and hydroxyl groups, forming a crystalline arrangement within chitosan (Almualla *et al.*, 2021). Introducing chitosan to the PVDF membrane yields a widening and intensification of the peak at 20°. Notably, the polyethylene-like structure of the PVDF β phase is evident through 2θ peaks at 21.3° and 23.7° (Borjigin *et al.*, 2013).

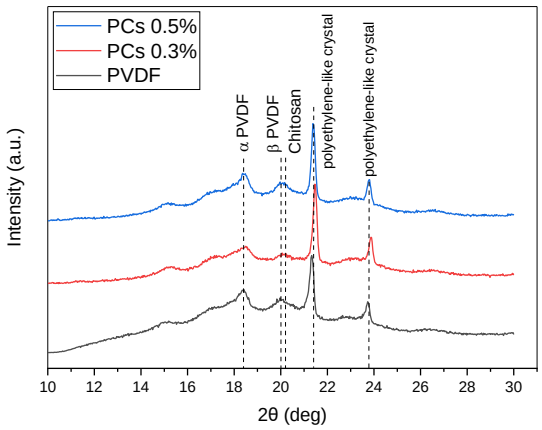

Figure 3. XRD diffractograms of the membranes.

The thermal stability of PVDF and PVDF/Chitosan membranes is shown by the TGA thermogram in Figure 4a. Upon the introduction of chitosan into the PVDF matrix, a degradation phase emerges within the temperature range of 50 – 150 °C, attributed to water evaporation (Tzaneva *et al.*, 2017). Notably, an increment in chitosan concentration correlates with an amplified release of water, reaching up to 12% upon 5% addition. The degradation of PVDF polymer matrix is marked by two distinct stages occurring within the temperature range of 420 – 675 °C (Jaleh *et al.*, 2015). The initial stage, observed within the 420 – 485 °C range, corresponds to the dehydrofluorination process involving the separation of F and H atoms from PVDF (Elsayeda *et al.*, 2022).

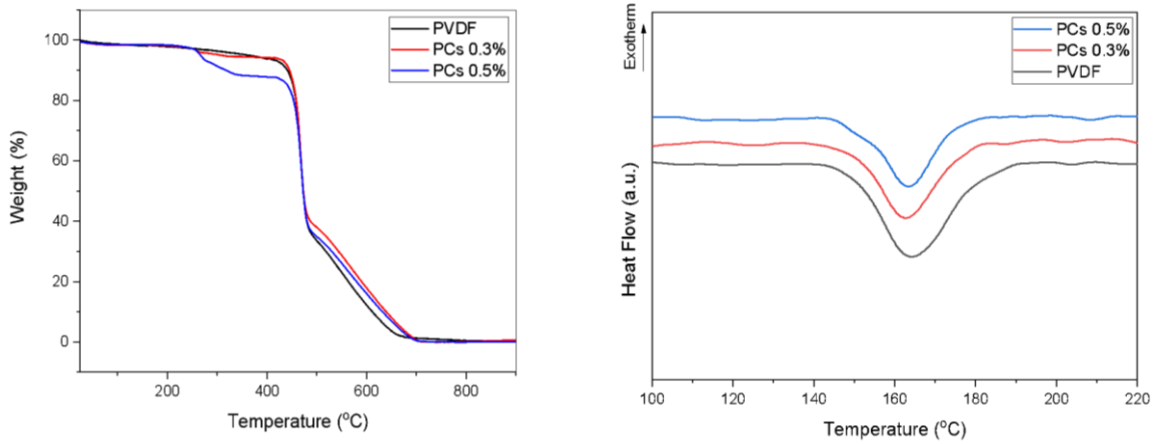

(a) (b)

Figure 4. Thermogram of (a) TGA and (b) DSC of the membranes.

Interestingly, PVDF with 0.3% and 0.5% chitosan additions exhibits the same first-stage degradation temperature of 420 °C. Subsequently, the second stage degradation, spanning 485 – 675 °C, corresponds to the main chain break of PVDF. Figure 4b, depicting the DSC thermogram, showcases the endothermic peak of the PVDF membrane at 164 °C. Intriguingly, the incorporation of chitosan does not substantially alter this endothermic peak. This implies that adding chitosan to the PVDF membrane fosters effective interaction without significantly affecting the PVDF melting point.

Hydrophilicity and Porosity Membranes

Analysis of membrane surface hydrophilicity was carried out by measuring the water contact angle shown in Figure 5a. The incorporation of chitosan led to a reduction in the contact angle of the PVDF membrane. This phenomenon signifies that adding chitosan to the PVDF/Chitosan membrane engenders heightened hydrophilicity, rendering the membrane surface more receptive to interaction with water molecules. The elevated β phase of PVDF, induced by chitosan, contributes to its increased hydrophilicity. Furthermore, the arrangement of chitosan atop the membrane surface promotes enhanced interactions with hydrophilic or amine groups, further augmenting the surface affinity for water molecules.

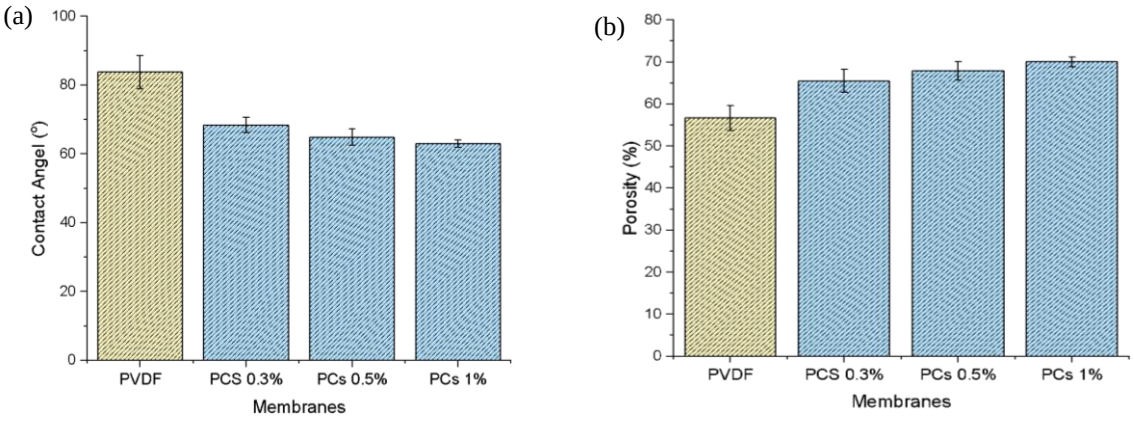

Figure 5. Graph of (a) Contact angle and (b) Porosity of the membranes.

The porosity of the membrane was determined by the gravimetric method shown in Figure 5b. The addition of chitosan increased the porosity of the PVDF membrane. Notably, the phase inversion method utilized during membrane fabrication inherently contributes to pore formation within the membrane. This is facilitated by the significant affinity contrast between the solvent and non-solvent systems, allowing for the rapid occurrence of demixing (Nawi *et al.*, 2020). The intricate interplay of polar-nonpolar interactions between chitosan and PVDF further influences the repulsion among polymer segments. This phenomenon subsequently fosters the creation of voids within the membrane structure, leading to a substantial enhancement in porosity.

Analysis of Membrane Surface and Cross-section

Surface and cross-section morphological analysis of PVDF and PCs 0.5% membranes were conducted by the SEM, as shown in Figure 6. On the surface of PVDF and PCs 0.5% membranes, there were no substantial distinctions. In general, the structures emerging on the membranes adopt an asymmetric composition characterized by a compact surface, a layer featuring finger-like formations, and a sponge-like structure. These formations arise due to the swift phase transition inherent to the process of phase inversion (Liu *et al.*, 2011; Lv *et al.*, 2018). Cross-sectional observations shown in Figure 6c and 6d indicate that the PVDF membrane exhibits relatively shorter finger-like macrovoids in comparison to 0.5% PCs. The finger-like macrovoid of PCs 0.5% membrane spans nearly the entire cross-sectional area. The presence of chitosan accelerates the exchange between the solvent and non-solvent (DMAc-water) during the phase inversion process. This, in turn, influences the formation of finger-like pore structures and the thickness of the membrane surface (Fathanah *et al.*, 2020).

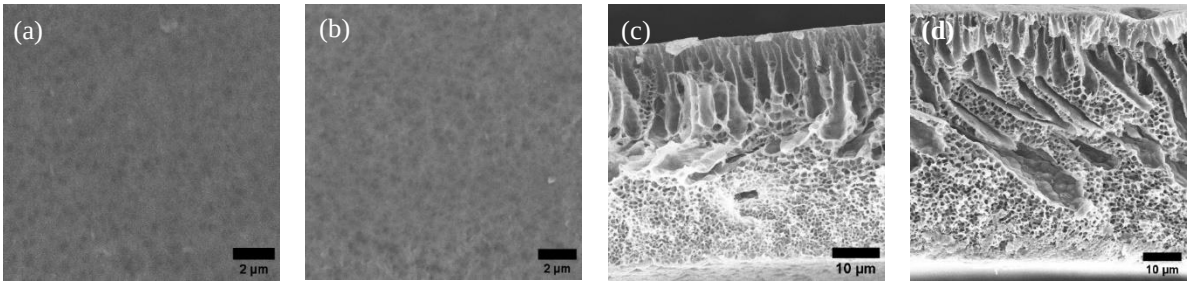

Figure 6. The SEM image of (a) PVDF membrane surface, (b) PCs 0.5% surface, (c) PVDF membrane cross section and (d) PCs 0.5% cross section.

Pure Water Flux Analysis

The effect of chitosan addition on the membrane pure water flux is shown in Figure 7. The data unequivocally demonstrates that the incorporation of chitosan results in an increase in pure water flux. For instance, the pure water flux of the PVDF membrane, initially at 28.32 L/m²h, escalates to 38.06 L/m²h with the addition of 1% chitosan. This augmentation signifies a remarkable 35% enhancement in the water flux of the PVDF membrane due to chitosan addition, reflecting favorable outcomes. The surge in membrane water flux aligns with the augmented hydrophilicity and porosity of the membrane. PVDF/Chitosan membrane surpasses the PVDF membrane in terms of water flux, mainly attributed to its heightened hydrophilicity. Simultaneously, the presence

of chitosan introduces increased pores within the PVDF membrane, facilitating smoother water passage through the membrane structure. The amine and hydroxyl groups of chitosan substitute foster hydrogen bonding with water molecules within the membrane. This interaction potential boosts the pure water flux value, as established by previous research (Lusiana *et al.*, 2017).

Analysis of Membrane Performance toward Filtration of Bovine Serum Albumin (BSA)

Membrane performance analysis was conducted by filtration of 100 mg/L BSA solution. BSA, a globular protein frequently employed as a laboratory-standard protein solution, was chosen for this purpose. The assessment of membrane performance concerning BSA filtration encompassed the determination of flux values and BSA rejection percentages, as depicted in Figure 8.

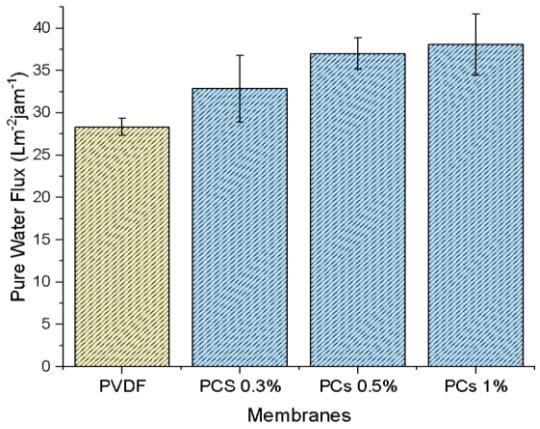

Figure 7. Pure water flux of the membranes.

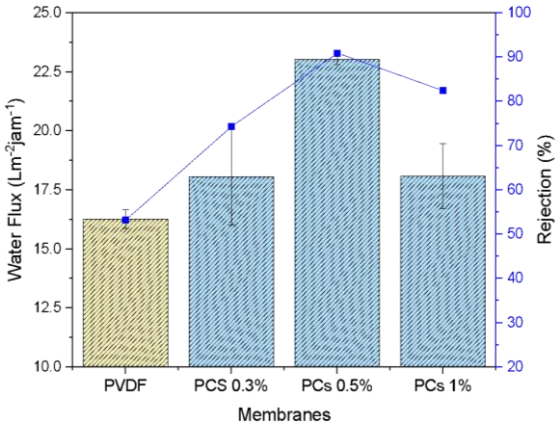

Figure 8. Membrane performance toward BSA filtration.

Incorporating chitosan into the membrane matrix yields heightened hydrophilicity, facilitating water permeation across the membrane. Intriguingly, the inclusion of 0.5% chitosan into the PVDF membrane engenders a notable increase in membrane selectivity, elevating the rejection percentage from 53% to 90%. However, the rejection of the PVDF membrane decreased with the addition of 1% chitosan. This phenomenon arises due to the arrangement of chitosan within the membrane pores. The substantial concentration of chitosan engenders robust interactions with proteins, thereby rendering it easier for proteins to permeate through the membrane. Consequently, this yields reduced flux and BSA rejection values as a consequence of increased protein permeation facilitated by the higher chitosan concentration. Hydrophobic polymers utilized as filtration membranes often grapple with the persistent issue of fouling. To counteract this challenge, elevating the membrane hydrophilicity has proven to be an effective strategy. The incorporation of chitosan into the PVDF membrane effectively heightens its hydrophilicity, consequently exerting a positive influence on its antifouling properties. The membrane antifouling attributes were assessed via the Flux Recovery Ratio (FRR) measurement, depicted in Figure 9.

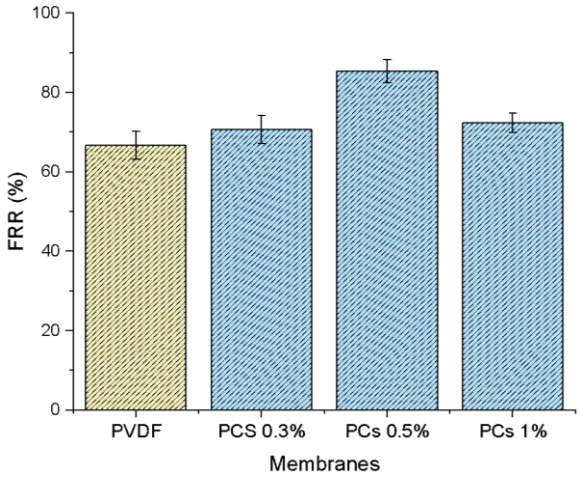

Figure 9. Antifouling properties of the membranes.

Remarkably, the inclusion of 0.5% chitosan led to a substantial increase in the FRR of the PVDF membrane, elevating it from 66% to 85%. This enhancement in FRR aligns seamlessly with the augmented hydrophilicity of the membrane, a finding that is well-supported by the data derived from water contact angle measurements.

The elevation in FRR value observed upon the introduction of chitosan to the PVDF membrane is attributed to the hydrophilic groups within chitosan, which facilitate the creation of a hydration layer on the membrane surface (An *et al.*, 2017). However, FRR decreased at the addition of 1% chitosan due to the interaction between chitosan and protein on the membrane surface. This interaction leads to the entrapment of proteins within the pores, making their release during the washing process arduous and consequently obstructing water passage through the membrane (Huang *et al.*, 2012).

To contextualize the results, a comparison of BSA rejection and FRR data from prior studies is presented in Table 2. The data clearly indicates that the modification with chitosan yields comparable outcomes with previous investigations, achieving a remarkable 90% BSA rejection and an FRR of 85.35%. While prior research has reported the highest FRR value reaching up to 97.92%, it has also noted relatively lower filtration performance at 68.19% (Fahrina *et al.*, 2021). These observations collectively affirm the significant potential of chitosan-modified PVDF membranes in advancing the protein filtration process.

Table 2. A comparative study of rejection and FRR of the PCs 0.5% with previous studies.

Membrane Filtration	Rejection (%)	FRR (%)	Reff
PVDF/GE-SiNPs	68.19	97.92	(Fahrina *et al.*, 2021)
PVDF/TiO_2-SPES	90.00	82.20	(Rahimpour *et al.*, 2011)
PVDF/CNC	88.20	84.00	(Lv *et al.*, 2018)
PVDF-g-PACMO	93.80	89.20	(Liu *et al.*, 2013)
PCs 0.5%	90.00	85.35	This work

The evaluation of membrane performance over the course of one hour, without undergoing any washing procedures, is shown in Figure 10a. Both the pure water flux and BSA flux values of PVDF membranes escalate with the addition of chitosan. This trend is in perfect alignment with the concurrent increase in membrane hydrophilicity and porosity, a phenomenon well-documented in the literature (Boributh *et al.*, 2009). As the analysis duration extends, however, the water flux undergoes a decline. This phenomenon stems from an accumulation of proteins on the membrane surface, resulting in fouling. This accumulation impedes the passage of water through the membrane and consequently diminishes the flux value.

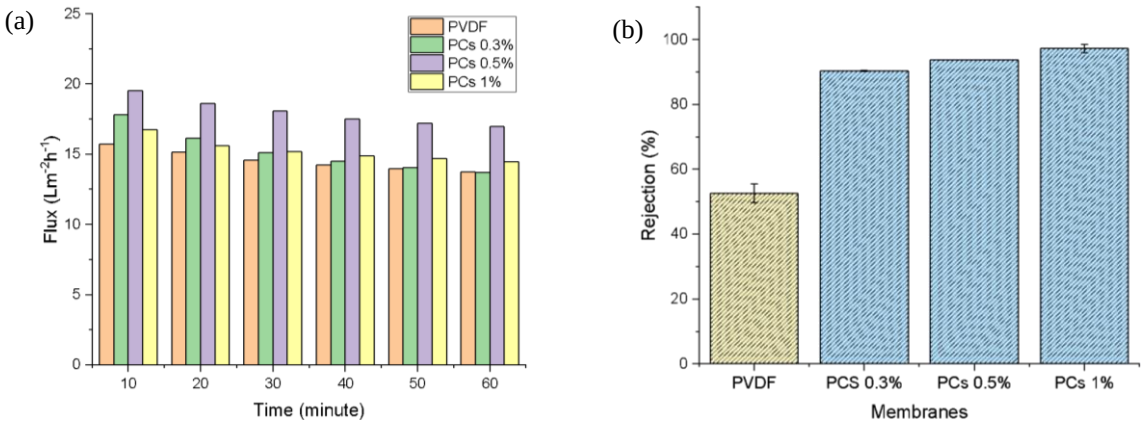

Figure 10. The analysis of (a) flux and (b) rejection after 60 minutes in continuous filtration using various membranes.

Additionally, the BSA rejection of the PVDF membrane following one hour of measurement exhibits an upward trajectory with the incorporation of chitosan, as shown in Figure 10b. The smaller water permeation rate results in heightened molecular rejection, a consequence of the augmented hydrophilicity of the membrane surface. This enhanced hydrophilicity effectively obstructs BSA molecules from traversing the membrane (Boributh *et al.*, 2009). the comprehensive analysis of membrane performance underscores the promising potential of chitosan-modified PVDF as a robust filtration membrane. This potential is substantiated by its high water flux, impressive >90% rejection rate, and commendable FRR, collectively affirming its viability for filtration applications.

CONCLUSION

This study has undertaken the utilization of chitosan as a filler material for PVDF membranes and subsequently conducted an in-depth performance analysis. The membranes were successfully fabricated using the phase inversion method with varying chitosan concentrations ranging from 0 to 1 wt%. The integration of chitosan led to an augmentation in the β fraction and an enhancement of hydrophilicity on the membrane surface. Notably, the highest β fraction attained was 68%, while the lowest contact angle measured was 63.03°, both achieved with a 1% chitosan addition. A proportional relationship emerged between chitosan concentration and membrane porosity, with the porosity rising from 56.64% to 70.02% for the 1% chitosan-infused PCs membrane. Membrane permeability exhibited a corresponding rise, as evidenced by the measurement of pure water flux reaching up to 38.06 L/m^2h, attributed to the heightened hydrophilicity imparted by chitosan. Performance evaluation of the membranes through the filtration of BSA solutions unveiled a remarkable rejection percentage exceeding 90% for the PVDF/Chitosan membrane. Furthermore, the temporal analysis of membrane performance exhibited an increase in both flux and rejection values upon the addition of chitosan, followed by a subsequent reduction with extended measurement duration. The FRR evaluation demonstrated that the PVDF membrane enriched with 0.5% chitosan outperformed its counterparts, marking the PCs 0.5% membrane as a highly promising contender for protein filtration applications.

CONFLICT OF INTEREST

There is no conflict of interest in this article.

AUTHOR CONTRIBUTION

RZ: Data Analysis, Methodology, and Wrote the Manuscript; AFN: Prepared Membranes and Analyzed the Membrane's Performance; YS: Tools Software and Visualization; ALP: Data Analysis and Visualization ; DVP: Membrane Analysis; DS: Visualization; MVI: Membrane Analysis and Visualization; WMN: Tools Software; WR: Introduction Drafting; OAS: Review the Manuscript; EP: Supervised the Experiment and Review the Manuscript. All authors agreed to the final version of this manuscript.

ACKNOWLEDGEMENTS

The authors would like to acknowledge the Directorate of Learning and Student Affairs (Belmawa)-Directorate General of Higher Education, Research and Technology (Ditjen Diktiristek) for providing financial support to this research through the Student Creativity Program for Exact Research (PKM-RE) 2022 No. 2489/E2/KM.05.01/2022.

REFERENCES

Abriyanto, H., 2021. 'Hydrophilic Modification of PVDF Membrane : a Review', *Journal of Membranes and Materials*, 1(1), 1–9. Available at: <https://ejournal2.undip.ac.id/index.php/jmm/article/view/10516.html>.

Al-Gharabli, S., Flanc, Z., Pianka, K., Terzyk, A. P., Kujawski, W., and Kujawa, J., 2023. Porcupine Quills-Like-Structures Containing Smart PVDF/Chitosan Hybrids for Antifouling Membrane Applications and Removal of Hazardous VOCs. *Chemical Engineering Journal*, *452*(2), 139281. https://doi.org/10.1016/j.cej.2022.139281.

Almualla, M., Mosa, M., and Sattar, M., 2021. Chemical Modification and Characterization of Chitosan for Pharmaceutical Applications. *Egyptian Journal of Chemistry*, *64*(7), 3635–3649. https://doi.org/10.21608/ejchem.2021.61809.3331.

An, Z., Xu, R., Dai, F., Xue, G., He, X., Zhao, Y., and Chen, L., 2017. PVDF/PVDF-g-PACMO blend hollow fiber membranes for hemodialysis: preparation, characterization, and performance. *RSC Advances*, *7*(43), 26593–26600. http://dx.doi.org/10.1039/C7RA03366D.

Ashok K, S., Srinivasan, G., and Govindaradjane, S., 2019. Development of a New Blended Polyethersulfone Membrane For Dye Removal From Synthetic Wastewater, *Environmental Nanotechnology, Monitoring and Management*, 12, 100238. https://doi.org/10.1016/j.enmm.2019.100238.

Azizati, Z., 2019. Pembuatan dan Karakterisasi Kitosan Kulit Udang Galah. *Walisongo Journal of Chemistry*, *2*(1), 10–16. https://doi.org/10.21580/wjc.v3i1.3878.

Boributh, S., Chanachai, A., and Jiraratananon, R., 2009. Modification of PVDF Membrane By Chitosan Solution For Reducing Protein Fouling, *Journal of Membrane Science*, 342(1–2), 97–104.

https://doi.org/10.1016/j.memsci.2009.06.022.

Borjigin, M., Eskridge, C., Niamat, R., Strouse, B., Bialk, P., and Kmiec, E. 2013. Electrospun Fiber Membranes Enable Proliferation of Genetically Modified Cells. *International Journal of Nanomedicine*, *8*, *855–864*. https://doi.org/10.2147/IJN.S40117.

Chong, J. Y., and Wang, R., 2019. From micro to nano: Polyamide thin film on microfiltration ceramic tubular membranes for nanofiltration. *Journal of Membrane Science*, *587*, 117161. https://doi.org/10.1016/j.memsci.2019.06.001.

Dong, H., Xiao, K., Tang, X., Zhang, Z., Dai, J., Long, R., and Liao, W., 2016. Preparation and Characterization of Polyurethane (PU)/Polyvinylidene Fluoride (PVDF) Blending Membrane. *Desalination and Water Treatment*, *57*(8), 3405–3413. https://doi.org/10.1080/19443994.2014.988659.

Elizalde, C. N. B., Al-Gharabli, S., Kujawa, J., Mavukkandy, M., Hasan, S. W., and Arafat, H. A., 2018. Fabrication of Blend Polyvinylidene Fluoride/Chitosan Membranes for Enhanced Flux and Fouling Resistance. *Separation and Purification Technology*, *190*, 68–76. https://doi.org/10.1016/j.seppur.2017.08.053.

Elsayeda, F. S., Abdulrahim, N. A., and Eladham, K. A., 2022. Studying of Thermal and Shielding Properties of PVDF (PolyVinyliDene Fluoride) Pipes Used in Aqueous Solution Sector. *Journal of Material Sciences and Manufacturing Research*, *3*(4), 1–6. https://doi.org/10.47363/jmsmr/2022(3)144.

Ezugbe, E. O., and Rathilal, S., 2020. Membrane Technologies in Wastewater Treatment: A Review. *Membranes*, *10*(5), 1–25. https://doi.org/10.3390/membranes10050089.

Fahrina, A., Yusuf, M., Muchtar, S., Fitriani, F., Mulyati, S., Aprilia, S., Rosnelly, C. M., Bilad, M. R., Ismail, A. F., Takagi, R., Matsuyama, H., and Arahman, N., 2021. Development of Anti-Microbial Polyvinylidene Fluoride (PVDF) Membrane Using Bio-Based Ginger Extract-Silica Nanoparticles (GE-Sinps) For Bovine Serum Albumin (BSA) Filtration. *Journal of the Taiwan Institute of Chemical Engineers*, *125*, 323–331. https://doi.org/10.1016/j.jtice.2021.06.010.

Fathanah, U., Machdar, I., Riza, M., Arahman, N., Lubis, M. R., and Yusuf, M., 2020. The Improvement of Hydrophilic Property of Polyethersulfone Membrane with Chitosan as Additive. *Jurnal Rekayasa Kimia and Lingkungan*, *15*(1), 53–61. https://doi.org/10.23955/rkl.v15i1.15916.

Fernandes-Queiroz, M., Melo, K., Sabry, D., Sassaki, G., and Rocha, H., 2014. Does the Use of Chitosan Contribute to Oxalate Kidney Stone Formation? *Marine Drugs*, *13*(1), 141–158. https://doi.org/10.3390/md13010141.

Gifuni, I., Lavenant, L., Pruvost, J., and Masse, A., 2020. Recovery of Microalgal Protein by Three-Steps Membrane Filtration: Advancements and Feasibility. *Algal Research*, *51*, 102082. https://doi.org/10.1016/j.algal.2020.102082.

Gregorio, R., 2006. Determination of the α, β, and γ Crystalline Phases of Poly(Vinylidene Fluoride) Films Prepared at Different Conditions. *Journal of Applied Polymer Science*, *100*(4), 3272–3279. https://doi.org/10.1002/app.23137.

Hassanzadeh, P., Gharbani, P., Derakhshanfard, F., and Memar Maher, B., 2021. Preparation and Characterization of PVDF/g-C_3N_4/Chitosan Polymeric Membrane for the Removal of Direct Blue 14 Dye. *Journal of Polymers and the Environment*, *29*(11), 3693–3702. https://doi.org/10.1007/s10924-021-02145-y.

Huang, J., Zhang, K., Wang, K., Xie, Z., Ladewig, B., and Wang, H., 2012. Fabrication of Polyethersulfone-Mesoporous Silica Nanocomposite Ultrafiltration Membranes With Antifouling Properties. *Journal of Membrane Science*, *423–424*, 362–370. https://doi.org/10.1016/j.memsci.2012.08.029.

Jaleh, B., Gavary, N., Fakhri, P., Muensit, N., and Taheri, S., 2015. Characteristics of PVDF Membranes Irradiated by Electron Beam. *Membranes*, *5*(1), 1–10. https://doi.org/10.3390/membranes5010001.

Japranata, H. H., 2016. *Separasi Protein dengan Membran Ultrafiltrasi*, *Teknik Kimia, Institut Teknologi Bandung*, Available at: <https://www.researchgate.net/publication/304483722_SEPARASI_PROTEIN_DENGAN_MEMBRAN_ULTRAFILTRASI> (accessed on July, 2023)

Junaidi, A. B., and Rahmadani, A., 2008. Efek Regenerasi Larutan Naoh Pada Deasetilasi Kitin Terhadap Derajat Deasetilasi Kitosan, 2(1), 36–43. http://doi.org/10.20527/jstk.v2i1.3890.

Kang, G. dong and Cao, Y. ming (2014) 'Application and Modification Of Poly(Vinylidene Fluoride) (PVDF) Membranes - A review', *Journal of Membrane Science*, 463, pp. 145–165. https://doi.org/10.1016/j.memsci.2014.03.055.

Khabibi, K., Siswanta, D. and Mudasir, M., 2021. Preparation, Characterization, and In Vitro Hemocompatibility of Glutaraldehyde-Crosslinked Chitosan/Carboxymethylcellulose as Hemodialysis Membrane, *Indonesian Journal of Chemistry*, 21(5), 1120–1131. https://doi.org/10.22146/ijc.61704.

Khajouei, M., Jahanshahi, M., and Peyravi, M., 2018. Biofouling Mitigation of TFC Membrane by In-Situ Grafting of PANI/Cu Couple Nanoparticle. *Journal of the Taiwan Institute of Chemical Engineers*, *85*, 237–247. https://doi.org/10.1016/j.jtice.2018.01.027.

Khan, T. A., Peh, K. K. and Ch'ng, H. S., 2002. Reporting Degree of Deacetylation Values of Chitosan: The Influence of Analytical Methods. *Journal of Pharmacy and Pharmaceutical Sciences*, 5(3), 205–212.

Khumalo, N. P., Vilakati, G. D., Mhlanga, S. D., Kuvarega, A. T., Mamba, B. B., Li, J., and Dlamini, D. S., 2019. Dual-Functional Ultrafiltration Nano-Enabled PSf/PVA Membrane For The Removal of Congo Red Dye. *Journal of Water Process Engineering*, *31*, 100878. https://doi.org/10.1016/j.jwpe.2019.100878.

Kou, S. (Gabriel), Peters, L. M., and Mucalo, M. R., 2021. Chitosan: A Review of Sources and Preparation Methods. *International Journal of Biological Macromolecules*, *169*, 85–94. https://doi.org/10.1016/j.ijbiomac.2020.12.005.

Liu, C., Wang, W., Li, Y., Cui, F., Xie, C., Zhu, L., and Shan, B., 2019. PMWCNT/PVDF Ultrafiltration Membranes With Enhanced Antifouling Properties Intensified by Electric Field for Efficient Blood Purification. *Journal of Membrane Science*, *576*, 48–58. https://doi.org/10.1016/j.memsci.2019.01.015.

Liu, F., Hashim, N. A., Liu, Y., Abed, M. R. M., and Li, K., 2011. Progress in the production and modification of PVDF membranes. *Journal of Membrane Science*, *375*(1), 1–27. https://doi.org/10.1016/j.memsci.2011.03.014.

Liu, J., Shen, X., Zhao, Y., and Chen, L., 2013. Acryloylmorpholine-Grafted PVDF Membrane with Improved Protein Fouling Resistance. *Industrial and Engineering Chemistry Research*, *52*(51), 18392–18400. https://doi.org/10.1021/ie403456n.

Lusiana, R. A., Putri Protoningtyas, W., Ricky Wijaya, A., Siswanta, D., Mudasir, M., and Juari Santosa, S., 2017. Chitosan-Tripoly Phosphate (CS-TPP) Synthesis Through Cross-linking Process: the Effect of Concentration Towards Membrane Mechanical Characteristic and Urea Permeation. *Oriental Journal of Chemistry*, *33*(6), 2913–2919. http://dx.doi.org/10.13005/ojc/330626.

Lusiana, R. A., Sangkota, V. D. A., Sasongko, N. A., Gunawan, G., Wijaya, A. R., Santosa, S. J., Siswanta, D., Mudasir, M., Abidin, M. N. Z., Mansur, S., and Othman, M. H. D., 2020. Permeability Improvement of Polyethersulfone-Polietylene Glycol (PEG-PES) Flat Sheet Type Membranes by Tripolyphosphate-Crosslinked Chitosan (TPP-CS) Coating. *International Journal of Biological Macromolecules*, *152*, 633–644. https://doi.org/10.1016/j.ijbiomac.2020.02.290.

Lv, J., Zhang, G., Zhang, H., Zhao, C., and Yang, F., 2018. Improvement of Antifouling Performances for Modified PVDF Ultrafiltration Membrane With Hydrophilic Cellulose Nanocrystal. *Applied Surface Science*, *440*, 1091–1100. https://doi.org/10.1016/j.apsusc.2018.01.256.

Munim, S. A., Saddique, M. T., Raza, Z. A., and Majeed, M. I., 2020. Fabrication of Cellulose-Mediated Chitosan Adsorbent Beads and Their Surface Chemical Characterization. *Polymer Bulletin*, *77*(1), 183–196. https://doi.org/10.1007/s00289-019-02711-4.

Nawi, M. N. I., Chean, H. M., Shamsuddin, N., Bilad, M. R., Narkkun, T., Faungnawakij, K., and Khan, A. L., 2020. Development of Hydrophilic PVDF Membrane Using Vapour Induced Phase Separation Method for Produced Water Treatment. *Membranes*, *10*(6), 1–17. https://doi.org/10.3390/membranes10060121.

Nunes, S. P., Culfaz-Emecen, P. Z., Ramon, G. Z., Visser, T., Koops, G. H., Jin, W., and Ulbricht, M., 2020. Thinking the future of membranes: Perspectives for Advanced and New Membrane Materials and Manufacturing Processes. *Journal of Membrane Science*, *598*, 117761. https://doi.org/10.1016/j.memsci.2019.117761.

Pishnamazi, M., Koushkbaghi, S., Hosseini, S. S., Darabi, M., Yousefi, A., and Irani, M., 2020. Metal Organic Framework Nanoparticles Loaded- PVDF/Chitosan Nanofibrous Ultrafiltration Membranes for The Removal of BSA Protein and Cr(VI) Ions. *Journal of Molecular Liquids*, *317*, 113934. https://doi.org/10.1016/j.molliq.2020.113934.

Pramono, E., Zakaria, M. A., Fridiasari, K. F., Ndruru, S. T. C. L., Bagaskara, M., Mustofa, R. E., Sejati, G. P. W., Purnawan, C., and Saputra, O. A., 2022. Cellulose Derived from Oil Palm Empty Fruit Bunches as Filler on Polyvinylidene Fluoride Based Membrane for Water Containing Humic Acid Treatment. *Groundwater for Sustainable Development*, *17*, 100744. https://doi.org/10.1016/j.gsd.2022.100744

Rahimpour, A., Jahanshahi, M., Rajaeian, B., and Rahimnejad, M., 2011. TiO2 Entrapped Nano-Composite PVDF/SPES Membranes: Preparation, Characterization, Antifouling And Antibacterial Properties. *Desalination*, *278*(1–3), 343–353. https://doi.org/10.1016/j.desal.2011.05.049.

Shahrabi, S. S., Barzin, J., and Shokrollahi, P., 2018. Blood Cell Separation by Novel PET/PVP Blend Electrospun Membranes. *Polymer Testing*, *66*, 94–104. https://doi.org/10.1016/j.polymertesting.2017.12.034.

Silitonga, R. S., Widiastuti, N., Jaafar, J., Ismail, A. F., Abidin, M. N. Z., Azelee, I. W., and Naidu, M., 2018. The Modification of PVDF Membrane via Crosslinking with Chitosan and Glutaraldehyde as the Crosslinking Agent. *Indonesian Journal of Chemistry*, *18*(1), 1–6. https://doi.org/10.22146/ijc.25127.

Thakur, P., Kool, A., Bagchi, B., Das, S., and Nandy, P., 2014. Enhancement of β Phase Crystallization and Dielectric Behavior of Kaolinite/Halloysite Modified Poly(Vinylidene Fluoride) Thin Films. *Applied Clay Science*, *99*, 149–159. https://doi.org/10.1016/j.clay.2014.06.025.

Trung, T. S., Thein-Han, W. W., Qui, N. T., Ng, C.-H., and Stevens, W. F., 2006. Functional Characteristics of Shrimp Chitosan and Its Membranes as Affected by The Degree of Deacetylation. *Bioresource Technology*, *97*(4), 659–663. https://doi.org/10.1016/j.biortech.2005.03.023.

Tzaneva, D., Simitchiev, A., Petkova, N., Nenov, V., Stoyanova, A., and Denev, P., 2017. Synthesis of Carboxymethyl Chitosan And Its Rheological Behaviour In Pharmaceutical And Cosmetic Emulsions. *Journal of Applied Pharmaceutical Science*, *7*(10), 70–78. https://doi.org/10.7324/JAPS.2017.71010.

Yusuf, A., Sodiq, A., Giwa, A., Eke, J., Pikuda, O., de Luca, G., di Salvo, J. L., and Chakraborty, S., 2020. A Review Of Emerging Trends In Membrane Science And Technology For Sustainable Water Treatment. *Journal of Cleaner Production*, *266*, 121867. https://doi.org/10.1016/j.jclepro.2020.121867.

Zhao, Y., Yang, W., Zhou, Y., Chen, Y., Cao, X., Yang, Y., Xu, J., and Jiang, Y., 2016. Effect Of Crystalline Phase On The Dielectric And Energy Storage Properties Of Poly(Vinylidene Fluoride). *Journal of Materials Science: Materials in Electronics*, *27*(7), 7280–7286. https://doi.org/10.1007/s10854-016-4695-y.

Zheng, L., Wang, J., Yu, D., Zhang, Y., and Wei, Y., 2018. Preparation of PVDF-CTFE Hydrophobic Membrane by Non-solvent Induced Phase Inversion: Relation Between Polymorphism and Phase Inversion. *Journal of Membrane Science*, *550*, 480–491. https://doi.org/10.1016/j.memsci.2018.01.013.